Structural Engineering and Mechanics, Vol. 8, No. 2 (1999) 137-150
DOI: http://dx.doi.org/10.12989/sem.1999.8.2.137

Numerical study on RC flat plates subjected to combined axial and transverse load

Honggun Park†

Department of Architecture, Seoul National University, San 56-1, Shinlim-Dong, Kwanak-Gu, Seoul 151-742, Korea

Abstract. This paper presents a numerical study on the flat plates in deep basements, subjected to floor load and in-plane compressive load due to soil and hydraulic lateral pressure. For nonlinear finite element analysis, a computer program addressing material and geometric nonlinearities is developed. The validity of the numerical model is established by comparison with existing experiments performed on plates simply supported on four edges. The flat plates to be studied are designed according to the Direct Design Method in ACI 318-95. Through numerical study on the effects of different load combinations and loading sequence, the load condition that governs the strength of the flat plates is determined. For plates under the governing load condition, parametric studies are performed to investigate the strength variations with reinforcement ratio, aspect ratio, concrete strength, and slenderness ratio. Based on the numerical results, the floor load magnification factor is proposed.

Key words: axial compression; finite element analysis; flat plate; reinforced concrete; slenderness; two-way slab.

1. Introduction

Recently in Korea, the construction of deep basements with up to 9 floors is increasing because of the high land price. The basements are usually used for parking and for mechanical and electrical purposes. The flat plate, a two-way slab system, is commonly used for the basement floor slabs. The basement structure with over 30 m depth below ground is subjected to large soil and hydraulic lateral pressure. The factored lateral load transferred to the flat plates in their 7th or 8th basement floor is 1500 to 3000 kN/m. As a result, the flat plates are subjected to not only the gravity load but also the in-plane compressive load due to the soil and hydraulic lateral pressure (See Fig. 1). The large in-plane compressive load is expected to cause the second-order effect on the flat plates.

For slender flat plates, therefore, it is necessary to consider the slenderness effect due to the in-plane compressive force. However, study on the flat plate subjected to the combined in-plane compressive and out-of-plane floor loads has not previously been reported. Current design codes do not provide the design provisions, either. Accordingly, most structural engineers design each strip of the flat plates as a continuous column. Although the flat plate under the in-plane and the out-of-plane loads is a compression member subjected to bending moment, the properties and the load conditions as well as the shape are different from those of columns in the following aspects:

† Assistant Professor

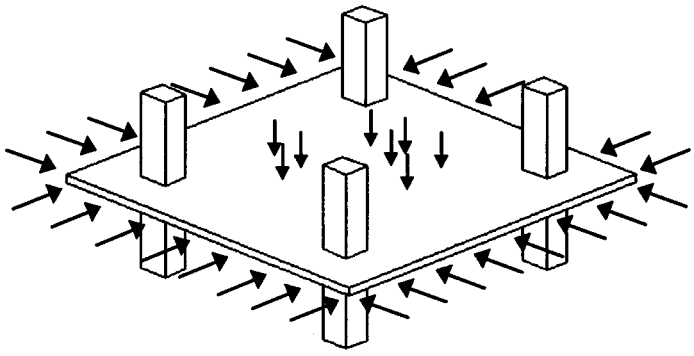

Fig. 1 Flat plate subjected to combined in-plane compressive and out-of-plane floor loads

1) Since the out-of-plane gravity load is irrelevant to the soil and hydraulic pressure inducing the in-plane compression, the loading sequence and the load combinations are arbitrary. Accordingly, the out-of-plane load is not proportional to the in-plane load. The out-of-plane gravity load may be applied to its full value before the in-plane load is applied.

2) The soil and hydraulic lateral pressure in one direction may be independent of that in the orthogonal direction. Accordingly, the flat plates could be subjected to either uniaxial or biaxial compressive load.

3) The ratio of span length to thickness, the slenderness ratio, is relatively uniform for most flat plates because current design codes specify the maximum slenderness ratio for deflection control. According to ACI 318-95 (American Concrete Institute 1995), for interior flat plates, the minimum thickness is $L_n/31$ to $L_n/36$, depending on the yield stress of reinforcing steel bars.

4) Reinforcement ratio is relatively low and is not uniform across the plate.

MacGregor and his colleague (Aghayere and MacGregor 1990a, b, Massicotte, MacGregor and Elwi 1991, Ghoneim and MacGregor 1994a, b) did experimental and/or numerical studies on reinforced concrete plates simply supported on four edges. Although study on the flat plates under in-plane compressive load has not been reported, the previous researches provide valuable knowledge about the behavior of the plates.

The main purpose of the presented study is to investigate the behavioral characteristics of slender flat plates subjected to in-plane and out-of-plane loads. For this purpose, a computer program for nonlinear finite element analysis of RC plates is developed. Parametric studies are performed to investigate the effects of different load combinations, loading sequence, reinforcement ratio, aspect ratio, concrete strength, and slenderness ratio on the behavior of the flat plates.

2. Numerical model

Three ingredients should be addressed in a numerical model for studying the behavior of slender plates subjected to the combined in-plane and out-of-plane loads. The material model should be able to address the strength enhancement under biaxial compression and the tensile cracking damage. The finite element should describe both the membrane and the plate-bending behavior. The finite element formulation should be adequate to present the second-order effect due to large deformation.

An existing computer program developed for plane stress problems (Park and Klingner 1997) is modified to accommodate shell elements and geometric nonlinearity. For material model of

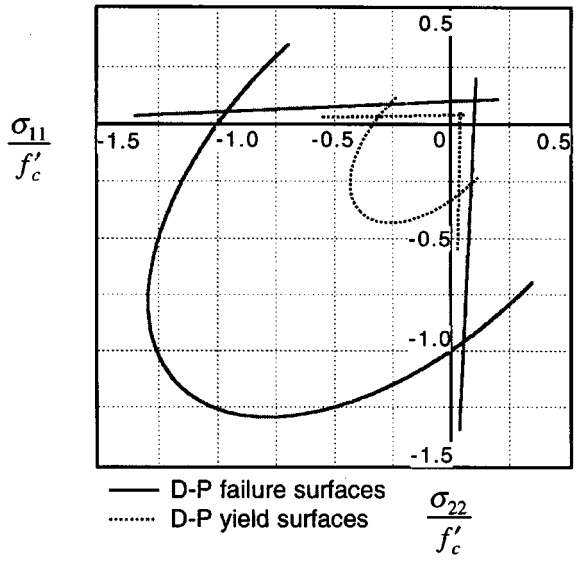

Fig. 2 Drucker-Prager failure surfaces in terms of plane stresses

reinforced concrete, the unified method combining plasticity theory and damage model is used. The concrete plasticity with multiple failure criteria addresses strength enhancement under multiaxial compression, and tensile cracking damage. The Drucker-Prager model is employed for the compressive and tensile failure criteria (See Fig. 2). Associative flow and isotropic hardening are used. In the analysis, 8-node shell elements are used to describe both the membrane and the plate-bending behavior. It is idealized that the reinforcing steel has smeared properties in the plane where the reinforcing steel layer is placed. Tension stiffening stress induced by the interaction between cracked concrete and reinforcing steel is idealized by a combination of tension softening and bond stresses. The bond stress is considered in the orientation of each reinforcement layer. The Updated Lagrangian Formulation is used for the geometric nonlinearity (Bathe 1982). At each loading step, the coordinates and the directional cosine vectors perpendicular to the tangent planes of the shell elements are updated by the corresponding displacements. The material model and the solution strategies for nonlinear computation are described in detail in the previous study (Park and Klingner 1997).

3. Verification of numerical model

As a preliminary study for flat plates, and for verifying the numerical model developed by the author, numerical study on plates simply supported on four edges is performed. Ghoneim and MacGregor (1994a, b) did experimental studies for the plates simply supported on four edges and subjected to the combined in-plane and out-of-plane loads. The experimental program for Plates C1, C2, C6, and C9 is summarized in Table 1. The plates have almost identical dimensions and properties, but have different load conditions. C1 is subjected to pure vertical load. C2 and C6 are subjected to combined in-plane compressive and vertical load. The in-plane load is applied first and kept constant while the vertical load is applied. C2 is subjected to uniaxial compressive load as the in-plane load while C6 is subjected to biaxial compressive load. On the other hand, C9 is

Table 1 Summary of experimental program for plates simply supported on four edges (Ghoneim and MacGregor 1994a, b)

Specimen	L_y mm	L_y/L_x	L_x/h	P_x kN/m	P_y kN/m	q kPa	f_c MPa	E_c MPa	ρ %
C1	1829	1.0	26.98	0.0	0.0	73.88	25.21	21300	0.383
C2	1829	1.0	27.06	0.0	653.9	52.59	25.27	21400	0.385
C6	1829	1.0	27.14	657.8	657.8	69.16	25.44	21720	0.386
C9	1829	1.0	27.34	0.0	342.4	52.50	24.94	19200	0.389

Note: F_y = 450 MPa, F_u = 620 MPa
Reinforcement is uniformly distributed at the top and the bottom in both directions.

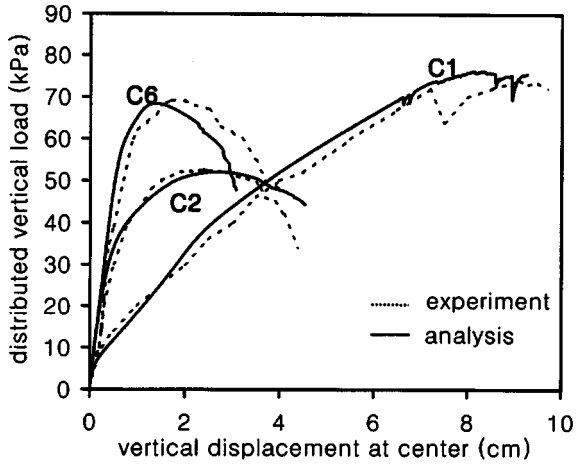

Fig. 3 Effect of different load combinations on plates simply supported on four edges

subjected to vertical load and subsequent uniaxial compressive load.

Fig. 3 compares the numerical and the experimental load-displacement curves for C1, C2, and C6 subjected to different load combinations. As shown in the figure, for all the plates, the numerical results agree well with the experimental ones. C1 has reduced stiffness due to flexural cracking at the beginning of the load-displacement curve. On the other hand, C2 and C6 have relatively large stiffness due to the in-plane compressive load. The in-plane compression affects the flexural strength of the plates in two opposite directions. It restraints the flexural cracking and enhances the flexural strength. On the contrary, the in-plane compression accompanied by the excessive out-of-plane deflections causes slenderness effect and consequently reduces the flexural strength. For C2 under uniaxial compressive load, the slenderness effect dominates, and the flexural strength decreases compared to that of C1. On the other hand, the strength of C6 under biaxial compressive load is larger than that of C2 under uniaxial compressive load. This is because concrete in biaxial compression shows enhanced compressive strength, and also the flexural strengths of the cross sections in both orthogonal directions increase.

C9 has a different loading sequence: vertical load and subsequent uniaxial compressive load (vertical-uniaxial load). Fig. 4 compares the experimental and the numerical results. The vertical load is applied first up to 52.5 kPa that is the vertical load capacity of C2 subjected to the uniaxial compressive load and the subsequent vertical load (uniaxial-vertical load). Then, the uniaxial load is increased until failure while the vertical load is kept constant. Ghoneim and

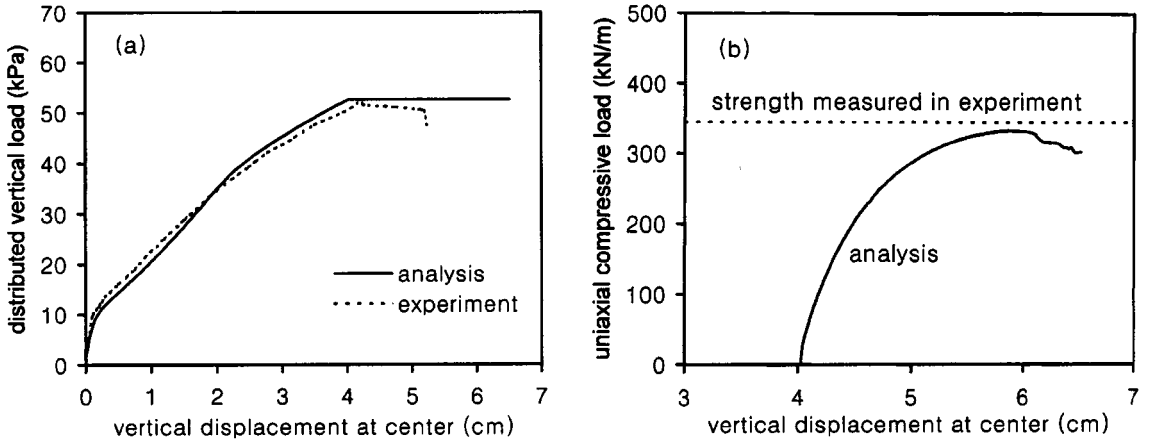

Fig. 4 Comparison of experiment and numerical results for C9 under vertical load and subsequently applied uniaxial Load: (a) vertical load-displacement curve; (b) uniaxial load-vertical displacement curve

MacGregor (1994b) reported that the uniaxial load capacity of C9 is 342.4 kN/m that is only half of the load capacity of C2 under the uniaxial-vertical load. As shown in Fig. 4, the numerical result agrees well with the experiment.

The effect of loading sequence on the strength of the plates is investigated in detail. The plates for investigation have the same properties as C1, but have different loading sequence, i.e., the uniaxial - vertical load and the vertical - uniaxial load. Fig. 5 compares the interaction curves of P/P_0 and q/q_0 for the plates with different loading sequence. P_0 is the pure uniaxial load capacity per unit length: $P_0 = f'_c\, h$. q_0 is the pure vertical load capacity per unit area, which is obtained by the numerical analysis. As shown in the figure, in the entire range of q/q_0, the strength of the plates under the vertical-uniaxial load is less than that under the uniaxial-vertical load. Difference in the strength is the most conspicuous in mid range of q/q_0.

For plates under the uniaxial-vertical load, the uniaxial compressive load restraints flexural cracking due to the vertical load applied subsequently. For plates under the vertical - uniaxial load, on the other hand, the prior application of the vertical load makes the cross sections cracked

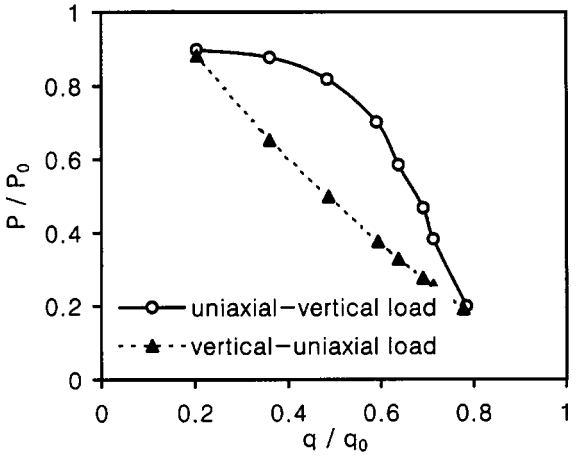

Fig. 5 Effect of loading sequence on plates simply supported on four edges

extensively. Accordingly, the uniaxial load accompanied by the reduced flexural stiffness and the large vertical deflection induces severe slenderness effect. Ghoneim and MacGregor (1994b) reported that the strength of the plates under the proportional vertical and uniaxial load is almost equal to that under the uniaxial-vertical load.

The study on the plates simply supported on four edges shows that the vertical-uniaxial load is the load condition that governs the strength of the plates, and also shows that the proposed numerical model is adequate to describe the behavior of the plates under combined in-plane and out-of-plane load.

4. Analytical program

The behavior of the flat plate is affected by various parameters such as boundary conditions, ratio of span length, and load conditions. In this paper, as a fundamental study for flat plates under in-plane load, a typical interior plate as shown in Fig. 1 is idealized with the following assumptions: 1) all plates have rectangular plans with the same span length in each direction; 2) shear failure does not occur; 3) columns do not provide any stiffness except supports in the vertical direction; and 4) all plates are subjected to uniformly distributed vertical and in-plane loads with the same magnitude so that they deflect downward and buckle simultaneously. The finite element model of the flat plate is shown in Fig. 6. Based on the assumptions noted above, a continuous flat plate system can be idealized as a plate with four corner columns. In addition, the plate can be reduced to a quarter model as shown in the figure.

The analytical program on the flat plates is summarized in Tables 2 and 3. The flat plates were designed in accordance with the Direct Design method recommended in ACI 318-95. The thickness of all the plates except PG, PJ, and PK series satisfies the requirement of the minimum thickness of two-way interior slabs, $L_n/33$. Arrangement of the reinforcing bars is also according to the design provisions for two-way slab construction. However, the bottom layers are arranged to be continuous in each strip of the plate.

5. Determination of governing load condition

Since the load combinations and the loading sequence are arbitrary as noted above, it is

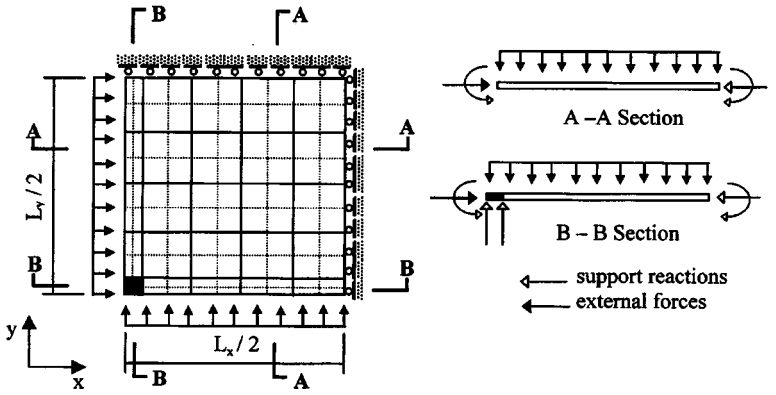

Fig. 6 Finite element model of flat plate

Table 2 Summary of analytical program for flat plates

Model	L_1 cm	L_2 cm	L_1/L_2	h cm	f_c MPa	E_c MPa	Load combination
PA1	600	600	1	17	24	23000	*V - U*
PA2	600	600	1	17	24	23000	*U - V*
PA3	600	600	1	17	24	23000	*V - B*[a]
PA4	600	600	1	17	24	23000	*B*[a] *- V*
PB1	900	600	1.5	25	24	23000	*V - U*
PB2	600	900	0.67	25	24	23000	*V - U*
PB3	900	600	1.5	25	24	23000	*V - B*[a]
PB4	900	600	1.5	25	24	23000	*V - B*[b]
PB5	900	600	1.5	25	24	23000	*V - B*[c]
PC1, PC2, PC3	600	600	1	17	24	23000	*V - U*
PD1, PD2, PD3	900	600	1.5	25	24	23000	*V - U*
PE1, PE2, PE3	1200	600	2	35	24	23000	*V - U*
PF1, PF2, PF3	600	900	0.67	25	24	23000	*V - U*
PG1, PG2, GP3	600	900	0.67	15	35	23000	*V - U*
PH1, PH2, PH3	600	600	1	17	24	28000	*V - U*
PI1, PI2, PI3	600	600	1	20	24	23000	*V - U*
PJ1, PJ2, PJ3	600	600	1	15	24	23000	*V - U*
PK1, PK2, PK3	600	600	1	13.5	24	23000	*V - U*

Note: Column size = 60 cm × 60 cm for 600 cm × 600 cm plates
= 80 cm × 80 cm for other plates
B - V: Biaxial compressive load and subsequently applied vertical load
V - B: Vertical load and subsequently applied biaxial compressive load
U - V: Uniaxial compressive load and subsequently applied vertical load (P_1:P_2 = 1:0)
V - U: Vertical load and subsequently applied uniaxial compressive load (P_1:P_2 = 1:0)
[a]P_1:P_2 = 1:1; [b]P_1:P_2 = 0.5:1; [c]P_1:P_2 = 1:0.5

Table 3 Reinforcement ratios for flat plates

Model	long span				short span				w kPa
	column strip		middle strip		column strip		middle strip		
	ends %	center %	ends %	center %	ends %	center %	ends %	center %	
PC1	0.483	0.201	0.155	0.133	0.483	0.201	0.155	0.133	11
PA series, PC2	1.040	0.412	0.315	0.270	1.040	0.412	0.315	0.270	22
PC3	1.647	0.615	0.467	0.399	1.647	0.615	0.467	0.399	32
PD1, PF1, PG1	0.480	0.200	0.154	0.132	0.283	0.120	0.075	0.075	11
PB series, PD2, PF2, PG2	1.025	0.410	0.314	0.269	0.586	0.243	0.092	0.079	22
PD3, PF3, PG3	1.610	0.611	0.464	0.397	0.884	0.358	0.135	0.116	32
PE1	0.431	0.183	0.141	0.121	0.183	0.078	0.075	0.075	11
PE2	0.924	0.373	0.286	0.245	0.374	0.157	0.075	0.075	22
PE3	1.429	0.554	0.423	0.362	0.555	0.230	0.075	0.075	32
PH1, PI1, PJ1, PK1	0.483	0.201	0.155	0.133	0.483	0.201	0.155	0.133	-
PH2, PI2, PJ2, PK2	1.040	0.412	0.315	0.270	1.040	0.412	0.315	0.270	-
PH3, PI3, PJ3, PK3	1.647	0.615	0.467	0.399	1.647	0.615	0.467	0.399	-

Note: Minimum reinforcement is 0.075% (= 0.15%/2) at the top and the bottom
Concrete cover + 1/2 diameter of a bar = 3 cm
F_y = 400 MPa, E_s = 210000 MPa, w = factored vertical load per unit area

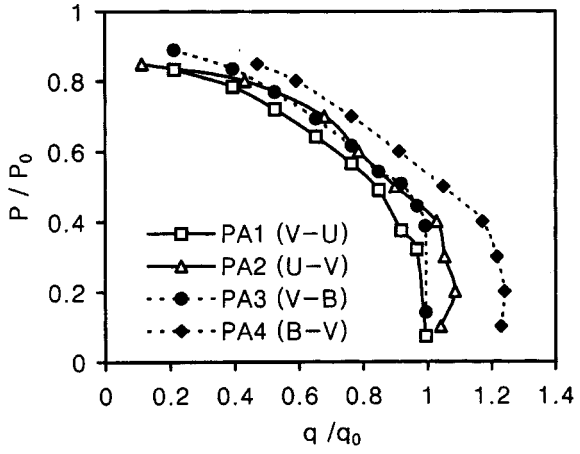

Fig. 7 Effect of load combinations and loading sequence on square flat plates

important to determine the load condition that governs the strength of the plate. Fig. 7 compares the interaction curves of P/P_0 and q/q_0 for square plates, PA series, under different load combinations and loading sequence. In the figure, *V-U, U-V, V-B* and *B-V* denote vertical-uniaxial, uniaxial-vertical, vertical-biaxial and biaxial-vertical loads, respectively. As shown in the figure, the strengths of PA1 and PA3 are larger than those of PA2 and PA4, respectively. This indicates that the prior application of the vertical load causes severe slenderness effect. It can also be observed that for the plates subjected to the vertical load first, the vertical load capacity, q, is not larger than the pure vertical load capacity, q_0. The interaction curves do not approach $P/P_0 = 1$ at $q/q_0 = 0$. This is because in the cross sections with different reinforcement ratios at the top and the bottom, the internal bending moment is induced by the axial force with eccentricity.

As also shown in the figure, PA1 subjected to the vertical load and the subsequent uniaxial compressive load (vertical-uniaxial load) has the least strength. This was observed also in the study on the plates simply supported on four edges (see Fig. 5). However, difference in strength of the flat plates is not so conspicuous as that of the plates simply supported on four edges. Since the flat plate is continuous and the edges where the distributed in-plane load is applied move downwards, difference between the deflections at the edges and the center is not so significant. Consequently, the slenderness effect is not so severe. Fig. 8(a) shows the deflected shape of PA1 at $q/q_0 = 0.966$.

Further, the effect of different load combinations is investigated for rectangular plates, PB series with the aspect ratio, $L_x/L_y = 1.5$. The PB series are subjected to the combined vertical and subsequent in-plane load. PB1 and PB2 are subjected to uniaxial compressive loads only, P_x and

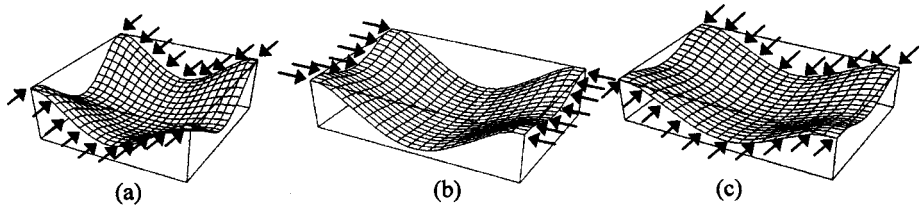

Fig. 8 Deformed shapes of (a) PA1 ($L_1/L_2 = 1$); (b) PB1 ($L_1/L_2 = 1.5$); (c) PB2 ($L_1/L_2 = 0.67$)

P_y, as the in-plane load. PB3, PB4 and PB5 are subjected to biaxial compressive loads with P_x/P_y = 1.0, 0.5 and 2.0, respectively. Fig. 9 compares the interaction curves for the PB series. As shown in the figure, generally, PB1 subjected to P_x only has the least strength. At low q/q_0, PB2 subjected to P_y only has the least strength. This indicates that in the entire range of q/q_0, the strength of the plate under the vertical-uniaxial load provides lower limit of strength. Figs. 8(b) and (c) show the deformed shapes of PB1 and PB2, respectively.

The study on the square and the rectangular flat plates under different load combinations and loading sequence shows that the vertical-uniaxial load is the governing load condition. This means that the plate designed for the vertical-uniaxial load is able to resist any combination of vertical load, and uniaxial or biaxial load.

6. Parametric study

For flat plates subjected to the vertical-uniaxial load that is the governing load condition, parametric studies are performed to investigate the strength variations of the plates with reinforcement ratio, aspect ratio, concrete strength, and slenderness ratio.

PC1, PC2, and PC3 were designed for the uniformly distributed vertical loads of 11, 22, and 32 kPa, respectively. The dimensions, properties, and reinforcement ratios are presented in Tables 2 and 3. Fig. 10 shows the interaction curves of P/P_0 and q/q_0. As shown in the figure, the interaction curves show similarity for the plates with different reinforcement ratios. Although PC1 with the least reinforcement ratio has the largest strength, the strength of PC3 with heavy reinforcement is not significantly less than that of PC1.

PC, PD, and PE series have different aspect ratios of L_1/L_2 = 1.0, 1.5, and 2.0, respectively, and they have almost identical slenderness ratios. PD and PE series are subjected to uniaxial load in the long span direction. Fig. 11 compares the interaction curves for PC2, PD2, and PE2. As shown in the figure, the interaction curves are not significantly affected by aspect ratios. This indicates that the plates with the same slenderness ratio have equivalent strength, regardless of the aspect ratios.

PF series are the companion plates of the PD series. The dimensions and properties of the PF

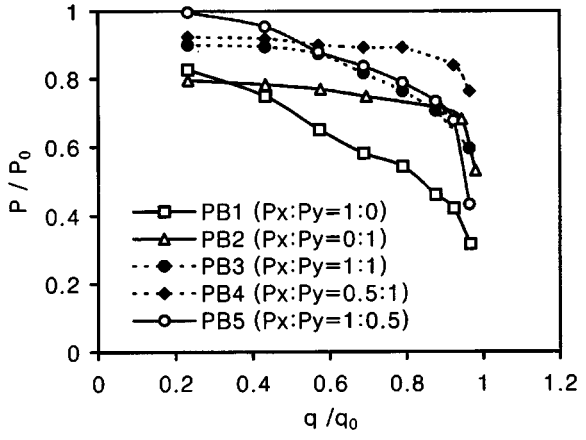

Fig. 9 Effect of different load combinations on rectangular flat plates (PB series with L_x/L_y=1.5)

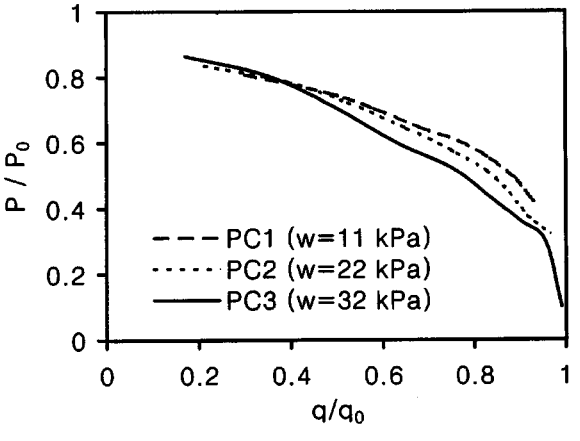

Fig. 10 Variations of interaction curve with reinforcement ratios

series are the same as those of the PD series, whereas the uniaxial load in the PF series is applied in the direction of the short span instead of the long span. Fig. 12 compares the interaction curves for PD and PF series. As shown in the figure, the strengths of PF2 and PF3 are larger than those of PD2 and PD3. Since the slenderness ratio with respect to the short span is less than that with respect to the long span, the slenderness effect is less significant for PD2 and PD3 under the uniaxial load in the short span. However, at high q/q_0, the strength of PF1 is less than that of PD1, which indicates that when the reinforcement ratio is very low, the strength of the plates under uniaxial load in the short span direction can be lower.

PH series have the same dimensions and properties as PC series except the concrete strength. The PH series use concrete of larger strength, f'_c=35 MPa. Fig. 13 compares the strength of the

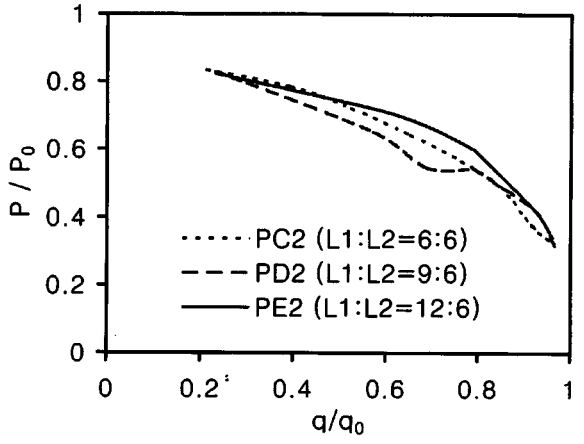

Fig. 11 Variations of interaction curve with aspect ratios

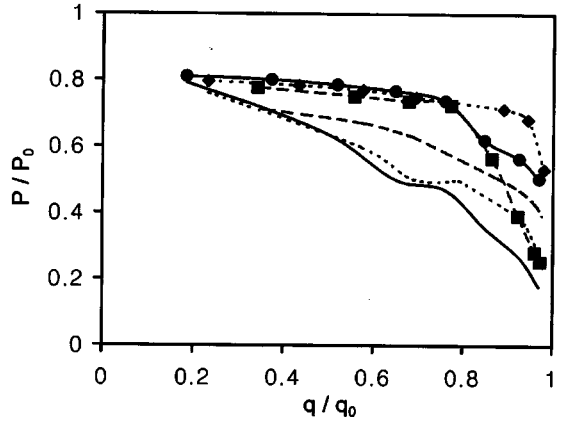

Fig. 12 Variations of interaction curve with direction of uniaxial load

PH and PC series. As shown in the figure, the plates with different concrete strength have comparable interaction curves.

PI, PC, PJ, and PK series were designed to have the thickness of 20, 17, 15 and 13.5 cms so that the slenderness ratios (L_1/h) are 30, 35, 40, and 44, respectively. Fig. 14 shows the variations of the interaction curve with the slenderness ratio. As shown in the figure, P/P_0 decreases as the slenderness ratio increases.

The numerical results from the parametric study show that the interaction curve of P/P_0 and q/q_0 is significantly affected by reinforcement ratio and slenderness ratio rather than aspect ratio and concrete strength.

7. Floor load magnification factor

Through the numerical studies performed above, the strength variations of the flat plates with reinforcement ratio, aspect ratio, concrete strength, and slenderness ratio are investigated. The numerical results are summarized in Fig. 15. Figs. 15 (a), (b) and (c) show the interaction of P/P_0 and q/q_0 for the plates with L_1/h 35, 30, and 44, respectively. The figures also show the proposed interaction curve that is the function of the slenderness ratio (L_1/h):

$$\left(\frac{P}{AP_0}\right)^B + \left(\frac{q}{q_0}\right) = 1 \tag{1}$$

where $A = -0.004\ (L_1/h) + 1.04$, and $B = -0.04\ (L_1/h) + 3.8$. P is the design uniaxial compressive load. P_0 is the axial load capacity of the plate that is approximately equal to $0.85f'_c\ h$. q is the design floor load, and q_0 is the pure floor load capacity of the plate. As shown in Fig. 15, the proposed interaction curve indicates the lowest of the numerical results. Also, it should be noted that the proposed interaction curve is applicable to the plates with L_1/h=30 to 44. As noted above, the interaction curve is affected by the reinforcement ratio as well. However, since the effect of

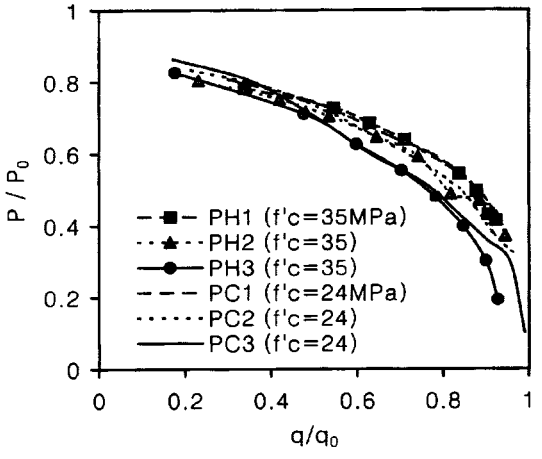

Fig. 13 Variations of interaction curve with concrete strength

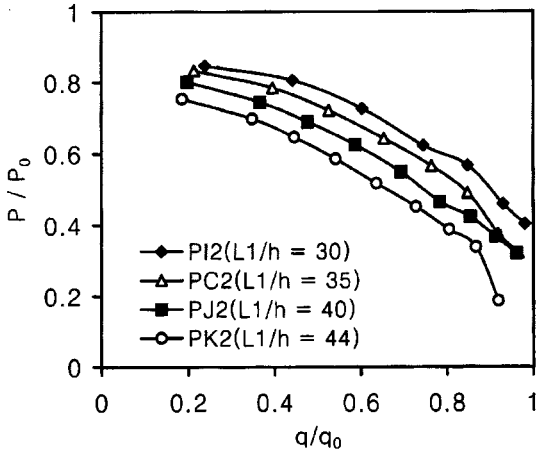

Fig. 14 Variations of interaction curve with slenderness ratio (L_1/h)

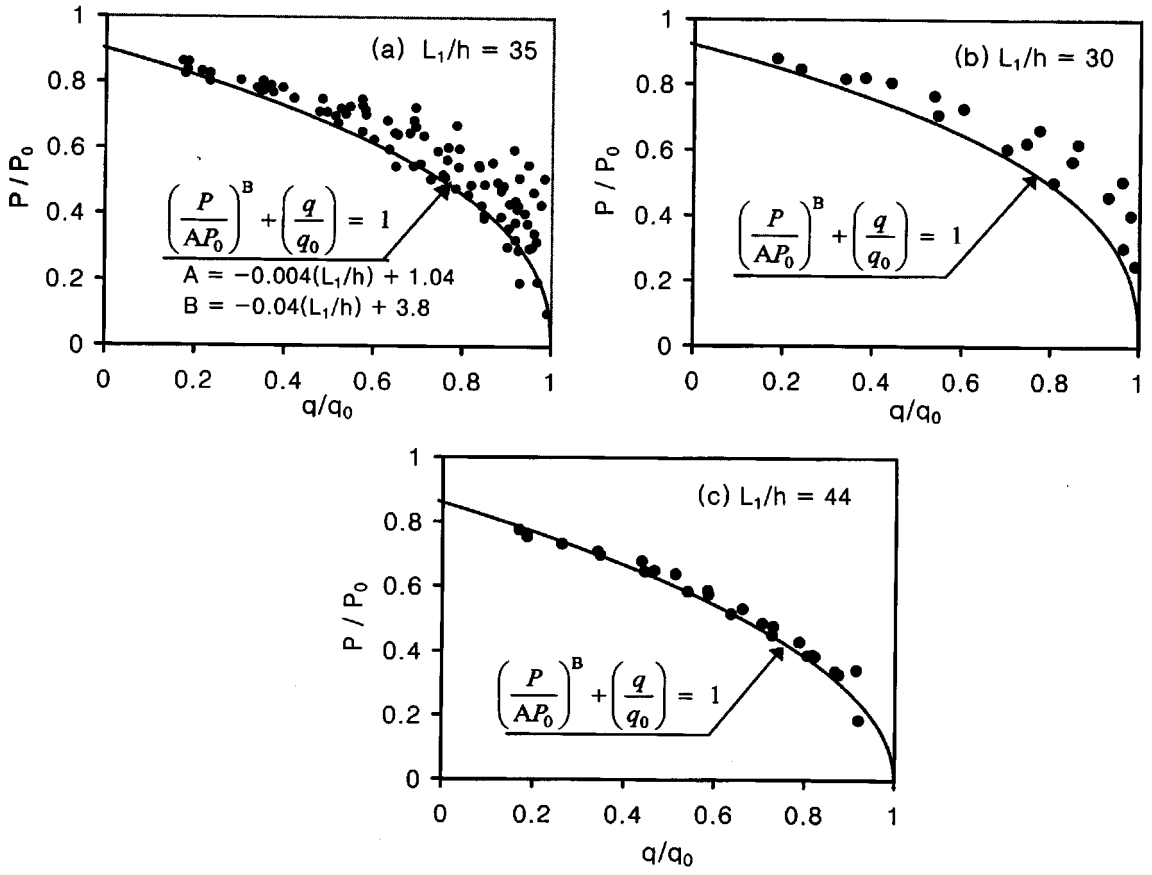

Fig. 15 Summary of analytical results and proposed interaction curve: (a) L_1/h = 35 (PC, PD, PE, and PH Series); (b) L_1/h = 30 (PI Series); (c) L_1/h = 44 (PK Series)

the reinforcement ratio on the strength depends on the direction of the uniaxial load (see Fig. 12), and since the reinforcement ratio is not uniform across the plate, it is difficult to define the interaction curve with a function of the reinforcement ratio.

As a design method for interior flat plates subjected to in-plane compressive load, the floor load magnifier method using the proposed interaction curve can be developed. With the known values of P, P_0, q and L_1/h, the pure floor load capacity, q_0, can be calculated from Eq. (1):

$$q_0 = \delta_q q, \text{ where } \delta_q = \frac{1}{1 - \left(\frac{P}{AP_0}\right)^B} \tag{2}$$

Table 4 Design example of square flat plates

L_1 cm	h cm	L_1/h	f'_c MPa	q kPa	P MN/m	P_0 MN/m	P/P_0	δ_q	q_0 kPa
600	17	35.3	24	20	2	4.08	0.49	1.31	26.2
900	25	36.0	24	20	2	6.00	0.33	1.10	22.0

in which δ_q is the floor load magnification factor. The flat plate can be designed as a flexural member under the pure floor load, q_0. It is not necessary to design the cross sections at different locations of the plate for combined axial compressive force and bending moment. However, this method is applicable only to the interior flat plates designed according to the Direct Design Method. Also, the creep effect on the magnification factor should be studied in the future.

Design examples for two square flat plates with different span length are presented in Table 4. The design compressive load, P, is 2 MN/m. The design floor load, q, is 20 kPa. The creep effect is not considered. As presented in the table, the plates with L_1=600 and 900 cm should be designed for the magnified floor loads, 26.2 and 22.0 kPa, respectively. As noted above, most flat plates are designed to satisfy the requirement of the maximum slenderness ratio for deflection control. Accordingly, as the span length increases, the thickness increases, and the plate has larger axial load capacity. Consequently, as presented in the table, the floor load magnification factor for the plate with long span length is less than that for the plate with short span length.

8. Conclusions

Numerical studies using nonlinear finite element analyses were carried out for investigating the behavior of the flat plates under combined floor load and in-plane compressive load. For the nonlinear finite element analyses, a computer program addressing material and geometric nonlinearities was developed. The numerical method was verified by comparison with the existing experiments performed on the plates simply supported on four edges.

The interior flat plates designed according to the Direct Design Method in ACI 318-95 were used as the analytical models. Since the load combinations and loading sequence are arbitrary, it is important to determine the load condition that governs the strength of the plates. The numerical study on the effects of different load combinations and loading sequence shows that the vertical load and the subsequent uniaxial load (vertical-uniaxial load) causes the most severe slenderness effect, and that it is the governing load condition.

For flat plates under vertical-uniaxial load, parametric studies were performed to investigate the variations of the interaction between P/P_0 and q/q_0 with reinforcement ratio, aspect ratio, concrete strength, and slenderness ratio. From the numerical results, it was observed that the interaction curve is significantly affected by reinforcement ratio and slenderness ratio rather than aspect ratio and concrete strength.

Based on the numerical results, the interaction curve of P/P_0 and q/q_0 that is the function of the slenderness ratio was proposed. As a design method for interior flat plates subjected to in-plane compressive load, the floor load magnifier method using the proposed interaction curve was developed. The floor load magnification factor is obtained from the proposed interaction curve. The flat plates can be designed as pure flexural members under the magnified floor load. This method is easy to use because it is not necessary to design the cross sections at different locations of the plate for the combined axial compressive force and bending moment. However, it is noted that application of this method is limited to continuous interior flat plates designed according to the Direct Design Method, which have uniform span length in each direction and are subjected to uniform vertical load. For general use of the floor load magnifier method, a broad range of parametric study should be performed.

The presented study provides only numerical results. Experimental research verifying the numerical results should be done in the future. Further research is needed to investigate creep

effect in flat plates under in-plane compression. The moment magnifier method that is applicable to the flat plates will be studied.

Acknowledgements

The author acknowledges the financial supports from Seoul National University under S.N.U Research Fund.

References

American Concrete Institute. (1995), "Building code requirements for structural concrete", *ACI 318-95*, Detroit, 118-121, 227-230.

Aghayere, A.O. and MacGregor, J.G. (1990a), "Analysis of concrete plates under combined in-plane and transverse Loads", *Structural J., ACI,* **87**(5), 539-547.

Aghayere, A.O. and MacGregor, J.G. (1990b), "Tests of reinforced concrete plates under combined in-plane and transverse Loads", *Structural J., ACI,* **87**(6), 615-622.

Bathe, K. (1982), *Finite Element Procedures in Engineering Analysis*, Prentice-Hall, Inc, 301-406.

Ghoneim, M.G. and MacGregor, J.G. (1994a), "Tests of reinforced concrete plates under combined inplane and lateral loads", *Structural J., ACI,* **91**(1), 19-30.

Ghoneim, M.G. and MacGregor, J.G. (1994b), "Behavior of reinforced concrete plates under combined inplane and lateral loads", *Structural J., ACI,* **91**(2), 188-197.

Massicotte, B., MacGregor J.G. and Elwi, A.E. (1991), "Behavior of concrete panels subjected to axial and lateral loads", *J. Struct. Engrg., ASCE,* **116**(9), 2324-2343.

Park, H. and Klingner, R.E. (1997), "Nonlinear analysis of RC members using plasticity with multiple failure criteria", *J. Struct. Engrg., ASCE,* **123**(5), 643-651.

Notations

E_c	elastic modulus of concrete
E_s	elastic modulus of reinforcing steel
F_y	yield stress of reinforcing steel
F_u	ultimate stress of reinforcing steel
f'_c	uniaxial strength of concrete
h	plate thickness
L_n	clear span length
L_1	length of span in the direction parallel to uniaxial load
L_2	length of span in the direction orthogonal to uniaxial load
L_x	length of span in x direction
L_y	length of span in y direction
P	applied uniaxial compressive load or design uniaxial load per unit length
P_x	applied uniaxial compressive load in x direction
P_y	applied uniaxial compressive load in y direction
P_0	uniaxial load capacity per unit length
q	applied vertical load or design vertical load per unit area
q_0	floor load capacity per unit area
w	factored vertical load per unit area
δ_q	floor load magnification factor
ρ	ratio of reinforcement area to gross concrete area